Observation of Quasimagnetic Structures in Rare-Earth-Based Icosahedral Quasicrystals

Benoît Charrier,[1] Bachir Ouladdiaf,[2] and Denys Schmitt[1]
[1]*Laboratoire de Magnétisme Louis Néel, CNRS, BP 166, 38042 Grenoble Cédex 9, France*
[2]*Institut Laue-Langevin, BP 156, 38042 Grenoble Cédex 9, France*
(Received 6 January 1997)

The first observation of long-range quasiperiodic antiferromagnetic structures in quasicrystals, namely the heavy rare-earth-based icosahedral $R_8Mg_{42}Zn_{50}$ compounds (R = Tb, Dy, Ho, Er), is reported. This *quasimagnetic* ordering is characterized by the propagation vector $\mathbf{Q} = (\frac{1}{4}, 0, 0, 0, 0, 0)$ in the six-dimensional notation. Simultaneously, broad magnetic peaks appear in the neutron diffraction patterns, characteristic of a short-range ordering. The coexistence of two different magnetic correlation lengths suggests the presence of two types of crystallographic sites for the rare-earth atoms. [S0031-9007(97)03306-1]

PACS numbers: 75.25.+z, 75.40.–s, 75.50.Kj

Quasicrystalline compounds have been found in many systems since their discovery in 1984 [1]. These so-called *quasicrystals* (QCs) present the remarkable property of exhibiting a long-range *orientational* order inconsistent with periodic translations. In particular, fivefold axes, characteristic of icosahedral symmetry and forbidden in conventional crystallography, can be observed in the diffraction patterns. A great number of studies have been dedicated to understanding the atomic ordering in QCs and a few structural models have been proposed [2]. On the other hand, many physical properties such as metallurgical, mechanical, and transport properties have been extensively investigated from an experimental as well as a theoretical point of view [3].

Most of the QCs observed up to now include a predominant proportion of aluminum and exist as metastable phases, i.e., can be obtained only by rapid solidification. Many of them contain potentially magnetic atoms such as Mn, Fe, Co, and Pd, but their magnetism in a quasicrystalline environment is very weak [4]. Moreover, the nature of the magnetism associated with these 3*d* or 4*d* elements is nonlocalized and carried by itinerant electrons, which makes its analysis in a nonperiodic structure difficult. In this respect, the investigation of rare-earth-based QCs appears particularly exciting because of the localized character of the 4*f* magnetic electrons. Few such systems have been discovered up to now and they have been little studied from a magnetic point of view. Icosahedral $R_8Mg_{42}Zn_{50}$ compounds, where R is a heavy rare earth (Gd to Er), have been the subject of more attention, being one of the few QCs not containing aluminum and presenting a stable quasicrystalline phase [5,6]. Thus, they offer the unique opportunity to study the magnetic behavior of localized 4*f* electrons in a nonperiodic structure. Initial magnetostatic studies revealed a spin-glass-like behavior with spin-freezing-like temperatures below 8 K [7]. Further studies revealed more details about the low temperature behavior giving evidence of giant geometrical frustration [8]: Indeed, large antiferromagnetic (AF) exchange interactions are present in this system but they seem to be *inhibited* by the nonperiodic structure. This suggestion was based on the fact that the transitions occur at much lower temperatures than expected when considering the paramagnetic Curie temperatures θ_p, i.e., $T_c \ll |\theta_p|$. Note that these critical temperatures (T_c = 5.8, 3.8, 2, and <1.5 K for R = Tb, Dy, Ho, and Er, respectively) correspond to the maximum of the dc susceptibility obtained after zero-field cooling. They also approximately correspond to the limit below which nonreversible effects are present on the magnetization curves.

We have carried out a detailed powder neutron diffraction study of *i*-$R_8Mg_{42}Zn_{50}$ compounds (R = Tb, Dy, Ho, Er) in order to have a deeper understanding of the actual behavior of the rare-earth magnetic moments in the low temperature phase. Experiments were performed on the multidetector diffractometer D1B at the Institut Laue-Langevin in Grenoble, by using a neutron wavelength $\lambda = 2.524$ Å. The samples were synthesized by induction melting in tantalum crucibles sealed under an argon atmosphere. They were then annealed by an appropriate thermal treatment [8]. X-ray powder diffraction patterns showed almost single phases as did the neutron diffraction patterns obtained in the paramagnetic phase [see, e.g., Fig. 1(a) for the Ho compound]. However, some weak extra peaks are present [see triangles in Fig. 1(a)] and correspond to the Mg_7Zn_3 phase as observed in other studies [9]. This latter phase contains no rare earth, ensuring that any magnetic contribution will be characteristic of the icosahedral phase alone. All the other diffraction peaks can be indexed according to the two-index scheme proposed by Cahn *et al.* for icosahedral systems [10]. In particular, the most intense observed peaks are similar to those observed by x rays, note the (18,29) and (20,32) peaks. The peaks are narrow and their width corresponds to the instrumental resolution [full width at half maximum (FWHM) = 0.6° for the (20,32) reflection]. The low temperature pattern of *i*-$Ho_8Mg_{42}Zn_{50}$ exhibits additional scattering of magnetic origin. The difference between the low and the high temperature patterns allows us to extract the magnetic

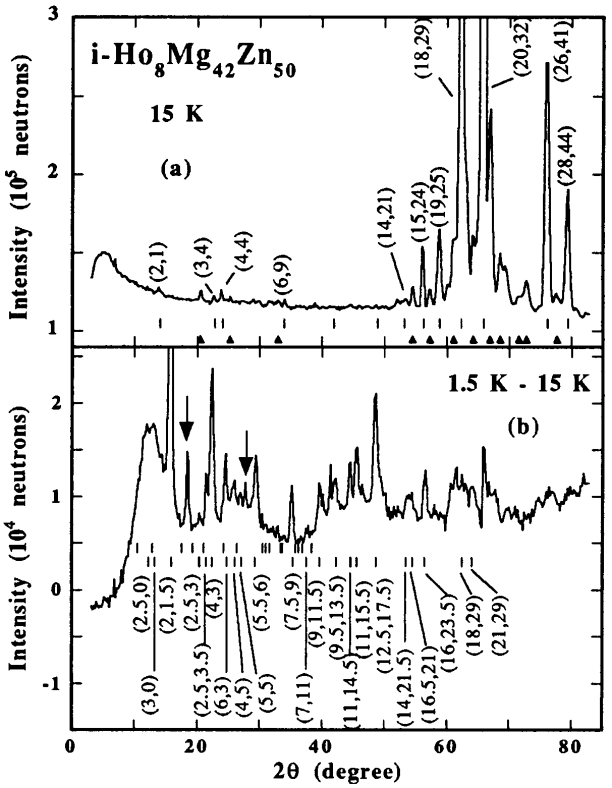

FIG. 1. (a) Neutron diffraction pattern for $Ho_8Mg_{42}Zn_{50}$ at 15 K; labels follow the two-index notation for nuclear reflections (see text); their position (vertical bars) is calculated for the hypercubic lattice constant $a_6 = 7.304$ Å; the triangles indicate the reflections of the Mg_7Zn_3 phase. (b) Difference between spectra obtained at 1.5 and 15 K; the labels (N, M) correspond to the strongest $(N_{\mathrm{mag}}, M_{\mathrm{mag}}) = (N + 0.125, M + 0.0625)$ magnetic reflections; $2\mathbf{Q}$ harmonics are indicated by the arrows.

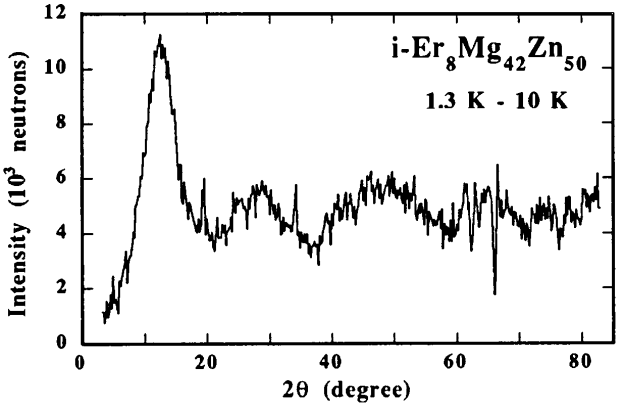

FIG. 2. Difference between low and high temperature spectra for $Er_8Mg_{42}Zn_{50}$.

contribution by removing the nuclear one. Two major features can be emphasized [see Fig. 1(b)]. First, a great number of narrow peaks, having a width similar to that of the nuclear peaks, are clearly observed in the whole angular domain, indicating the presence of a *long-range magnetic ordering* for the rare-earth magnetic moments. Secondly, another more diffuse scattering can be observed, as shown by the successive broad peaks centered around $2\theta = 12$, 26, and 45° (FWHM $\approx 6°$ for the first peak), and suggests the presence of *short-range magnetic correlations.* The coexistence of two different magnetic correlation lengths appears quite surprising and will be discussed below. The same behavior occurs in the four compounds studied, although the specific features depend on the rare earth involved, as shown in Fig. 2. In fact, two groups of compounds can be distinguished. On one hand, the Tb and Ho spectra are similar, showing strong narrow magnetic peaks together with weaker broad magnetic peaks. On the other hand, in the Dy and Er patterns, the long-range contribution is very small, and the main contribution originates from the short-range ordering. Explaining this subdivision would be premature at this stage and will require a more quantitative analysis. It should be mentioned, however, that, contrary to Tb and Ho, Dy and Er are Kramers-type atoms, so that the rules of degeneracy for the rare-earth crystal-field levels (they are necessarily doublets in Dy and Er) could be involved in the phenomenon.

Several neutron diffraction patterns were collected in the temperature range 1.3–20 K in order to follow the temperature dependence of both types of magnetic contribution. As an example, the variation for some selected integrated peaks is reported in Fig. 3 for $Tb_8Mg_{42}Zn_{50}$. Obviously, both short- and long-range magnetic order vanishes at the same critical temperature, i.e., $T_N \approx 20$ K. Here, the label T_N (for Néel temperature) is used because of the *antiferromagnetic* nature of the long-range ordering (see below). This intimate connection between both variations can be considered as a strong evidence that both contributions are *intrinsic* to the quasicrystalline compound and do not arise from distinct parts of the samples. The other, surprising result is that T_N is about *3 times higher* than the critical temperature T_c obtained from macroscopic magnetic measurements (see above). The only anomaly occurring around T_N on the dc susceptibility curve is that a slight deviation from its Curie-Weiss behavior becomes perceptible below T_N (inset of Fig. 3). On the other hand, a slight increase of intensity of the narrow magnetic Bragg peaks is visible around T_c. The same behavior is observed in the other compounds, where the vanishing of the neutron diffraction peaks occurs at $T_N = 12$, 7, and 5 K for Dy, Ho, and Er compounds, respectively.

The first step in the quantitative analysis of the long-range magnetic contribution consists in *indexing* the diffraction diagram, i.e., finding a coherent set of indexes for all the narrow magnetic peaks. In a way reminiscent of the description of magnetic structures in conventional crystals, where all the magnetic diffraction peaks can be generated from one three-dimensional propagation vector, we tried to find such a unique vector $\mathbf{Q}$ in the six-dimension reciprocal space commonly used in the

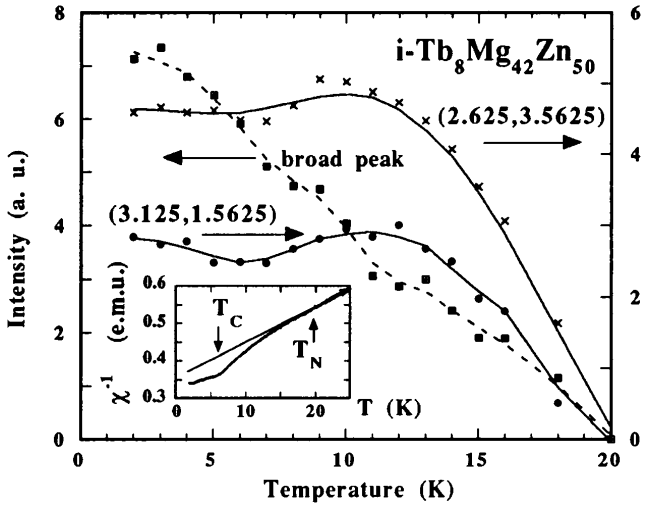

FIG. 3. Temperature variation of the first broad peak at $2\theta = 12°$ (left scale) and the two (2.625, 3.5625) and (3.125, 1.5625) narrow peaks (right scale) in $Tb_8Mg_{42}Zn_{50}$; lines are guides for the eyes. Inset: temperature dependence of the reciprocal susceptibility (the straight line is the extrapolation of the high temperature part).

description of QC powder diffraction data [10]. Note that in $R_8Mg_{42}Zn_{50}$ compounds the reciprocal lattice is body-centered hypercubic [11]. The simple propagation vector $\mathbf{Q} = (\frac{1}{4}, 0, 0, 0, 0, 0)$ has been found to satisfy the required conditions: Each observed magnetic reflection corresponds to at least one (generally numerous) vector $\mathbf{q} = \mathbf{Q} + \mathbf{K}$, where $\mathbf{K}$ is a reciprocal lattice vector and its angular position is related to the length of the scattering vector $\mathbf{q}_\parallel$ which is the projection of $\mathbf{q}$ into the three-dimension reciprocal space. Following the alternative two-index scheme [10], we can also adopt the same short notation $(N_{\mathrm{mag}}, M_{\mathrm{mag}})$ as for the nuclear peaks (N, M). Nevertheless, N_{mag} and M_{mag} are no longer integers because of the fractional part of $\mathbf{Q}$ [see Fig. 1(b)]. For example, in the Ho compound, the strongest magnetic reflection ($2\theta = 15.90°$) corresponds to $\mathbf{q} = (0.25, 1, 0, 0, 0, 0)$, i.e., $(N_{\mathrm{mag}}, M_{\mathrm{mag}}) = (2.125, 1.5625)$. Only two narrow peaks do not enter in this indexing, namely for $2\theta = 18.35$ and $28.35°$ [arrows in Fig. 1(b)]. However, both peaks can be related to the second harmonic $2\mathbf{Q}$, corresponding to (0.5,1,0,0,0,0) and (0.5,0,1,1,0,0), respectively. The fact that all the magnetic peaks can be indexed within a *unique* scheme starting from a single propagation vector $\mathbf{Q}$ is strong evidence for the quasiperiodic origin of the magnetic diffraction, i.e., for the existence of a *quasimagnetic* structure. Moreover, this latter is an *antiferromagnetic* one, since the unit cell of the direct hypercubic lattice must be *quadrupled* along the (1,0,0,0,0,0) direction to account for the magnetic quasiperiodicity. Describing more precisely the arrangement of the magnetic moments now requires a specific model to be developed, allowing us to calculate the intensity of each reflection, that will be considered later.

To give a first idea of what a *quasiperiodic antiferromagnetic* order can be, we may focus on the one-dimensional Fibonacci sequence. Assuming a simple AF structure with $\mathbf{Q} = (\frac{1}{2}, 0)$ in the corresponding two-dimensional square lattice means that each node is *colored* with the $+$ or $-$ attribute (for *up* or *down* magnetic moments, respectively) giving rise to the $+-+-+-$ sequence along the x axis. Projecting onto the one-dimensional real space [2] leads to assign the $+$ or $-$ *color* to the L and S segments of the initial Fibonacci sequence. This results in the new nonperiodic sequence $L^-S^-L^+L^-S^-L^+S^+L^-L^+S^+\ldots$ based on *four* distinct elements (L^+, L^-, S^+, S^-) instead of two. This situation then appears wealthier than the previous one and new types of local rules must be considered. For example, in the same way that the SS pairs are forbidden in the Fibonacci chain, the six pairs $L^+L^+, L^-L^-, L^+S^-, L^-S^+, S^+L^+, S^-L^-$ are forbidden in the AF Fibonacci chain. Giving more details is beyond the scope of the present study, but wide developments may be anticipated in this respect.

We now focus our attention on the short-range magnetic correlations. We chose the Er compound because the corresponding contribution is easier to extract from the data (Fig. 2). This contribution has been obtained by removing all the narrow peaks remaining in the difference pattern. The radial correlation function $g(r)$ can be calculated by Fourier transforming the experimental data [12]

$$g(r) = \int_{q_{\min}}^{q_{\max}} I_{\mathrm{diff}}(q) f(q)^{-2} q \sin(qr)\, dq\,,$$

where $I_{\mathrm{diff}}(q)$ is the diffuse magnetic scattering intensity at q and $f(q)$ is the magnetic form factor (here we use q for the modulus of $\mathbf{q}_\parallel$). The integration covers the range ($0.15-3.2$ Å^{-1}) but smaller $q_{\max}$ values have been also considered to check the consistency of the calculated $g(r)$ (see Fig. 4). In the absence of any quantitative information about the relative positions of the atoms in $R_8Mg_{42}Zn_{50}$ QCs, the following conclusions must be taken with care and will have to be confirmed independently. Since the radial correlation function is a sum of spin-spin correlations for all pairs of magnetic atoms in the limit of isotropic interactions, any significative extremum should be associated with a well defined distance between Er atoms. Considering that the low-r region ($r < \sim 3$ Å) is meaningless and the high-r one ($r > \sim 10$ Å) is not reliable (due to cut-off effects), it can be concluded that three preferential nearest-neighbour (NN) distances between Er atoms seem to be present in the $Er_8Mg_{42}Zn_{50}$ quasicrystal, namely around 5.2, 7.2, and 8.7 Å (arrows in Fig. 4). For the third NN distance, the pair coupling is the strongest and negative, in good agreement with the overall AF properties. A fourth distance could be present around 3.9 Å, corresponding to a large ferromagnetic pair coupling, but, being at the limit of jointed atomic spheres, it must be considered with care.

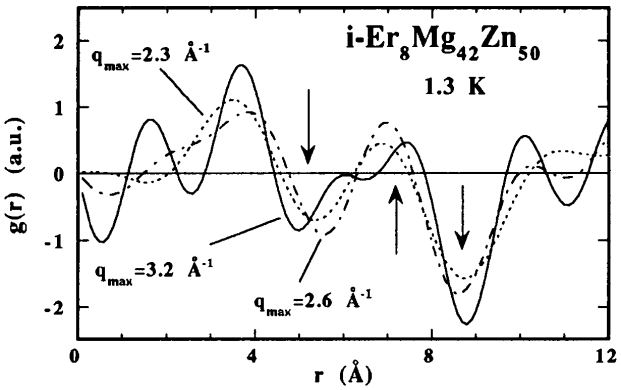

FIG. 4. Radial correlation function in $Er_8Mg_{42}Zn_{50}$ at 1.3 K; different lines correspond to different choices for the upper q-integration limit; arrows indicate the first three preferential nearest-neighbor distances between rare-earth atoms.

The coexistence of two correlation lengths in $R_8Mg_{42}Zn_{50}$ quasicrystals suggests two different types of rare-earth sites. The first group of sites should perfectly satisfy the icosahedral symmetry, because it is the only way to produce a coherent long-range elastic diffraction consistent with narrow peaks. The second group of rare-earth atoms would be partially disordered: In fact, the existence of preferential distances suggests an assembly of ordered sites having well defined positions but with an occupation number smaller than unity, i.e., they are randomly occupied to fit the exact proportion of rare earth in the structure. Such a distribution of rare-earth positions should then be seen in the nuclear scattering amplitudes as well. The two correlation scales are reminiscent of low-dimensional systems where different strengths of coupling exist between and within magnetic planes, for example. Here, however, both assemblies of sites are intimately and three-dimensionally overlaping, so that a noticeable correlation subsists between them. That could explain the simultaneity of both long- and short-range ordering temperatures. An alternative explanation for the short-range contribution could be the existence of a partially disordered magnetic component. A third possibility could be related to the phason disorder which has been shown to be present in other QCs leading to diffuse scattering located close to the Bragg reflections [13]. Such phason defects associated to a fraction of the rare-earth sites could explain the impossibility for those magnetic moments to order on a long-range scale. The correlation length of the diffuse magnetic scattering can be estimated to be around 25 Å from the width of the first broad peak. However, the exact meaning of this length as well as the link between the preferential distances given above and the possible phason strain remain to be elucidated.

The absence of a clear anomaly in the susceptibility or heat capacity curves at T_N remains to be explained as well as the spin-glass-like behavior. It should be noted that spin freezing phenomena have been recently observed in site-ordered systems such as the pyrochlore antiferromagnet $Tb_2Mo_2O_7$ [14] or gadolinium gallium garnet [15]. In these systems, the geometric frustration of the building blocks (triangles or tetrahedra) prevents the spins being ordered at low temperature. One can imagine that the icosahedral structure is another case of a geometrically frustrated lattice leading to specific unusual magnetic properties as observed in the $R_8Mg_{42}Zn_{50}$ quasicrystals.

To conclude, it is worth noting that, for the first time, a long-range quasiperiodic antiferromagnetic structure has been clearly shown to occur in a quasicrystalline material. It can be emphasized that the rare-earth atoms appear as privileged probes for the investigation of the icosahedral structure through their magnetic properties. Further studies are now necessary to quantitatively account for the actual arrangement of the magnetic moments in these quasimagnetic structures, to understand how these latter are linked to the macroscopic magnetic properties and to explain the differences from one compound to another.

[1] D. Shechtman, I. Blech, D. Gratias, and J. W. Cahn, Phys. Rev. Lett. **53**, 1951 (1984).
[2] C. Janot, in *Quasicrystals, a Primer* (Clarendon Press, Oxford, 1992).
[3] See *Quasicrystals*, edited by C. Janot and R. Mosseri (World Scientific, Singapore, 1995).
[4] R. C. O'Handley, R. A. Dunlap, and M. E. McHenry, Philos. Mag. B **61**, 677 (1990).
[5] Z. Luo, S. Zhang, Y. Tang, and D. Zhao, Scr. Metall. **28**, 1513 (1993).
[6] A. P. Tsai, A. Niikura, A. Inoue, T. Masumoto, Y. Nishida, K. Tsuda, and M. Tanaka, Philos. Mag. Lett. **70**, 169 (1994).
[7] Y. Hattori, A. Niikura, A. P. Tsai, A. Inoue, T. Masumoto, K. Fukamichi, H. Aruga-Katori, and T. Goto, J. Phys. Condens. Matter **7**, 2313 (1995).
[8] B. Charrier and D. Schmitt, J. Magn. Magn. Mater. (to be published).
[9] Z. P. Luo, H. X. Sui, and S. Q. Zhang, Metall. Mater. Trans. A **27**, 1779 (1996).
[10] J. W. Cahn, D. Schechtman, and D. Gratias, J. Mater. Res. **1**, 13 (1986).
[11] A. Niikura, A. P. Tsai, A. Inoue, and T. Matsumoto, Philos. Mag. Lett. **69**, 351 (1994).
[12] E. F. Bertaut and P. Burlet, Solid State Commun. **5**, 279 (1967).
[13] M. de Boissieu, M. Boudard, B. Hennion, R. Bellissent, S. Kycia, A. Goldman, C. Janot, and M. Audier, Phys. Rev. Lett. **75**, 89 (1995).
[14] B. D. Gaulin, J. N. Reimers, T. E. Mason, J. E. Greedan, and Z. Tun, Phys. Rev. Lett. **69**, 3244 (1992).
[15] P. Schiffer, A. P. Ramirez, D. A. Huse, P. L. Gammel, U. Yaron, D. J. Bishop, and A. J. Valentino, Phys. Rev. Lett. **74**, 2379 (1995).